


RESEARCH ARTICLE

The potential role of hsa_circ_0001079 in androgenetic alopecia via sponging hsa-miR-136-5p

Hanxiao Wei¹ | Xiaoyu Xu²  | Shuai Yang² | Chang Liu² | Qiang Li¹ | Peisheng Jin¹

¹Department of Plastic Surgery, Affiliated Hospital of Xuzhou Medical University, Xuzhou, China

²Xuzhou Medical University, Xuzhou, China

Correspondence

Peisheng Jin, Department of Plastic Surgery, Affiliated Hospital of Xuzhou Medical University, No.99, Huaihai Street, Xuzhou 221000, Jiangsu, China.
Email: jinps2006@163.com

Abstract

Background: Androgenetic alopecia (AGA) is an androgen-dependent polygenic hereditary disease.

Methods: Diseased hair follicles from 5 AGA patients and normal hair follicles from 5 healthy individuals were selected as specimens to carry out whole transcriptome sequencing. Multiple high-expression circular RNAs (circRNAs) were screened from the diseased group. We further verified the presence of the circRNAs in the clinical specimens by real-time fluorescence quantitative PCR (qRT-PCR).

Results: In total, 100 circRNAs were significantly upregulated, and 184 circRNAs were significantly downregulated. The top 10 upregulated circRNAs were hsa_circ_0101041, hsa_circ_0001578, hsa_circ_0135062, hsa_circ_0002980, hsa_circ_0005062, hsa_circ_0072688, hsa_circ_0133954, hsa_circ_0001079, hsa_circ_0005974, hsa_circ_0000489. The top 10 downregulated circRNAs were hsa_circ_0001278, hsa_circ_0031482, hsa_circ_0008285, hsa_circ_0003784, hsa_circ_0077096, hsa_circ_0001148, hsa_circ_0006886, hsa_circ_0000638, hsa_circ_0084521, and hsa_circ_0101074. Among top 10 upregulated circRNAs, hsa_circ_0001079 showed significantly high expression via large-sample verification and clinical application potential. Based on a database comparison and base pairing analysis, we found that has-miR-136-5p bound to hsa_circ_0001079 and that hsa-miR-136-5p had potential binding sites with Wnt5A.

Conclusion: In summary, through high-throughput sequencing and bioinformatic analysis, a potential diagnostic marker for alopecia and a key circRNA that might adsorb microRNA (miRNA) through a sponging mechanism, thus mediating alopecia, were discovered in this study.

KEYWORDS

androgenetic alopecia, biomarker, hsa_circ_0001079, hsa-miR-136-5p, sponging, Wnt5A

Hanxiao Wei and Xiaoyu Xu contributed equally to this work and should be considered to share first authorship.

This is an open access article under the terms of the Creative Commons Attribution-NonCommercial-NoDerivs License, which permits use and distribution in any medium, provided the original work is properly cited, the use is non-commercial and no modifications or adaptations are made.

© 2021 The Authors. *Journal of Clinical Laboratory Analysis* published by Wiley Periodicals LLC.

1 | INTRODUCTION

Androgenetic alopecia (AGA), also known as seborrheic alopecia, is an androgen-dependent polygenic hereditary disease. For young patients with a clear family history of genetic diseases, premature hair loss seriously affects their physical and mental health. During the course of AGA, irreversible shrinkage, a shortened growth period and a prolonged resting period of the hair follicle ultimately lead to the loss of the ability to regenerate hair.^{1,2} At present, there are many treatments for AGA, such as the oral administration of finasteride tablets, the topical application of minoxidil and hair transplant surgery, etc.³ In recent years, the injection of platelet-rich plasma (PRP)^{4,5} or autologous fat⁶ and even novel drug delivery systems have emerged.⁷ Although the treatment methods are constantly improving, AGA can still not be cured effectively.⁸ Therefore, the fundamental methods to treat AGA still rely on a deep understanding of the pathogenesis of AGA and the exploration of the pathological transformation process of dermal papilla cells during hair follicle growth and development.

Circular RNAs (circRNAs) is a newly discovered category of RNA that widely exists in human body, which can be divided into noncoding circRNAs and coding circRNAs.^{9,10} CircRNAs have a unique covalent closed loop structure that makes these molecules difficult to degrade by exonucleases and debranching enzymes and have good biological stability and tissue and cell specificity.¹¹ CircRNAs can regulate gene expression through multiple mechanisms, the most common of which is the large number of binding sites with sponging miRNAs, thus reducing the inhibitory effect of miRNA on target gene expression by competitively binding with miRNA.¹² Studies have shown that circRNAs play important roles in tumours,¹³ cardiovascular diseases,¹⁴ immune system diseases, etc.^{15,16} However, the role of circRNAs in AGA is still unclear.

In this study, the differential circRNA expression profiles of hair follicles from AGA patients and healthy individuals were screened by high-throughput whole transcriptome sequencing, and the possible mechanism by which circRNAs affect the pathogenesis of AGA was investigated. We found that the expression of hsa_circ_0001079 was significantly higher in AGA patients than in healthy individuals, a finding that was further confirmed by qRT-PCR via large-sample verification in the AGA group. Receiver operating characteristic curve (ROC) analysis indicated that hsa_circ_0001079 was of great value in the diagnosis of AGA, suggesting that hsa_circ_0001079 is a potential clinical diagnostic marker of alopecia. Further bioinformatic analysis revealed that hsa_circ_0001079 might adsorb has-miR-136-5p to regulate cell functions through a sponging mechanism. This study provides a novel diagnostic marker and therapeutic target for AGA.

2 | MATERIALS AND METHODS

2.1 | Specimen collection

A total of 30 untreated male AGA patients and 30 healthy male volunteers signed informed consent forms. In this study, hair follicles from 5 AGA patients and 5 healthy individuals were randomly selected for

sequencing. The patients provided written informed consent, and the study was approved by the Institutional Review Board of Xuzhou Medical College Affiliated Hospital (Jiangsu, China).

2.2 | Extraction of RNA and quality control

A Trizol reagent kit was used to extract RNA from hair follicle tissue, and a NanoDrop ND-2000 instrument was used to determine the RNA concentration. The OD260/OD280 value was used to assess RNA purity. CircRNA was enriched and pretreated using a CircRNA Enrichment Kit to generate a sequencing library. Furthermore, quality was also tested.

2.3 | RNA library preparation and high-throughput sequencing

This work was performed by CloudSeq Biotech (Shanghai, China). A TruSeq whole-stranded RNA library preparation kit (Illumina) was used for RNA pretreatment and sequencing library construction. Quality control and library quantification were carried out using a Bio-Analyzer 2100 system (Agilent Technologies, Santa Clara, CA, USA). High-quality sequencing was conducted using a reference genome/transcriptome and STAR software (v2.5.1b).

2.4 | Identification of circRNAs and function prediction

CircRNAs with significantly differential expression were considered those with a fold-change R of 2.0 and $p < 0.05$. Gene ontology (GO) and Kyoto Encyclopedia of Genes and Genomes (KEGG) analyses were performed on related genes of circRNAs with significant differential expression to predict the functions of these circRNAs. Using each circRNA with its miRNA binding site and the predicted miRNA site data, an interaction network between each circRNA and its downstream miRNA was constructed using Cytoscape software (v2.8.0).

2.5 | Real-time fluorescence quantitative PCR verification

Total RNA was extracted from hair follicle tissue using Trizol (Invitrogen, Carlsbad, CA USA), and cDNA was synthesized using a ReverTraAc real-time qPCR kit (Toyobo, Osaka, Japan). After the reaction, product purity was assessed based on the melting curve, and the Cq value was obtained by statistical processing in Rq Manager analysis software. The relative expression of RNA in each specimen was calculated using the $2^{-\Delta\Delta Ct}$ method. Three replicates were conducted for all specimens, and the average value was used for analyses.

2.6 | Luciferase reporter assay

Wnt5A wild-type and mutant-type luciferase reporter vector targeting the hsa-miR-136-5p binding site were constructed. The vectors and hsa-miR-136-5p mimics were co-transfected into cells by Lipofectamine 2000 reagent, and luciferase activities were measured 24 h later using the dual luciferase reporter system (Promega, USA). Renilla luciferase activity was used as a standardized control.

2.7 | Statistical analysis

SPSS 17.0 statistical software was used for the statistical analysis. The quantitative data are expressed as the mean \pm SD. The *t* test was adopted for comparisons between the 2 groups, and differences were considered statistically significant when $p < 0.05$. GraphPad software (San Diego, USA) was used to manage and analyze the data.

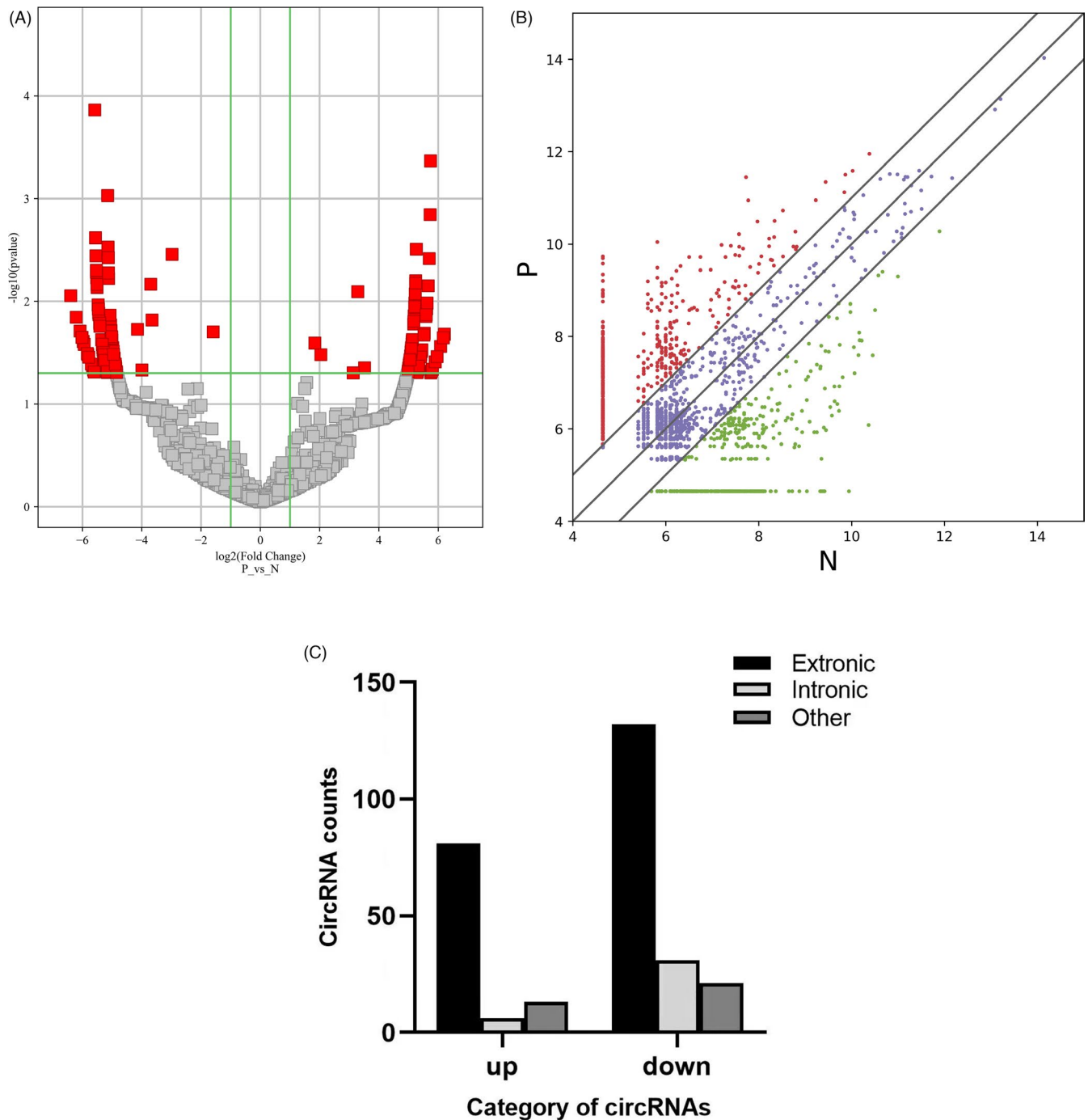
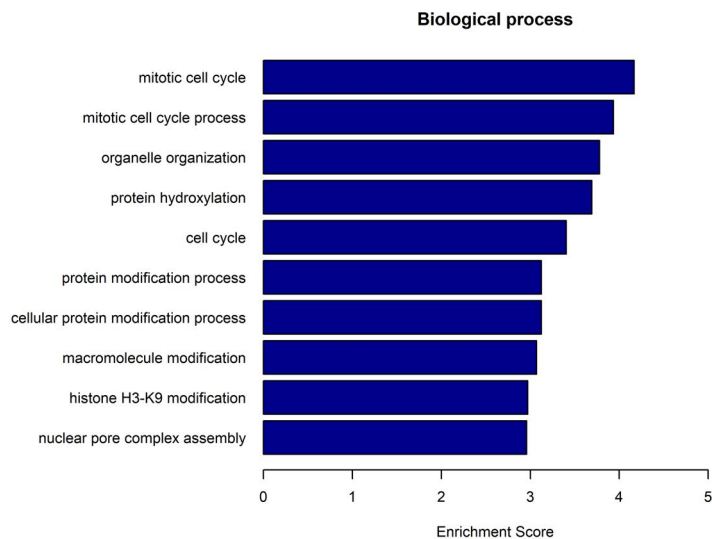


FIGURE 1 Differentially expressed circRNAs between AGA patients and healthy controls (A) Volcano plot showing the differential expression of circRNAs between AGA patients and healthy controls (NC). The red blocks represent circRNAs with statistically significant differences in expression. (B) In the cluster heatmap, the red line represents upregulated circRNAs, and the green line represents downregulated circRNAs. (C) Among the 284 circRNAs with significant differential expression, 100 were significantly upregulated, and 184 were significantly downregulated

TABLE 1 Information of 20 differentially expressed circRNAs

CircRNA ID	Host gene	logFC	logCPM	P value	Regulation
hsa_circ_0101041	DNAJC3	5.967795285	9.19948445	0.034563517	Up
hsa_circ_0001578	RANBP9	5.901422954	9.15571504	0.038900565	Up
hsa_circ_0135062	ANKIB1	5.804078356	9.09275692	0.04585028	Up
hsa_circ_0002980	AGK	5.744649651	9.055078873	0.000430647	Up
hsa_circ_0005062	KANK1	5.732000007	9.046804627	0.001433234	Up
hsa_circ_0072688	ADAMTS6	5.702196733	9.028195527	0.003843978	Up
hsa_circ_0133954	RAPGEF5	5.664737455	9.004925185	0.007065064	Up
hsa_circ_0001079	STK39	5.628815803	8.982247148	0.010407945	Up
hsa_circ_0005974	CAPRN1	5.613751985	8.973353937	0.011870219	Up
hsa_circ_0000489	RNASEH2B	5.596812397	8.962776192	0.013522704	Up
hsa_circ_0001278	STT3B	-6.396681953	9.489706328	0.008847093	Down
hsa_circ_0031482	HECTD1	-6.080093049	9.266977324	0.019518921	Down
hsa_circ_0008285	CDYL	-6.016852414	9.224148891	0.022473411	Down
hsa_circ_0003784	SPG11	-5.974390698	9.192451266	0.024616833	Down
hsa_circ_0077096	SENP6	-5.941206402	9.172304783	0.026299849	Down
hsa_circ_0001148	SRSF4	-5.55969559	8.929293383	0.002414419	Down
hsa_circ_0006886	ZCCHC2	-5.529001057	8.910640484	0.005216071	Down
hsa_circ_0000638	POLI	-5.512911066	8.902328652	0.006860037	Down
hsa_circ_0084521	LUC7L2	-5.506194293	8.896968242	0.007372751	Down
hsa_circ_0101074	FAM192A	-5.449522253	8.863749284	0.013046563	Down



GO Biological Process Classification

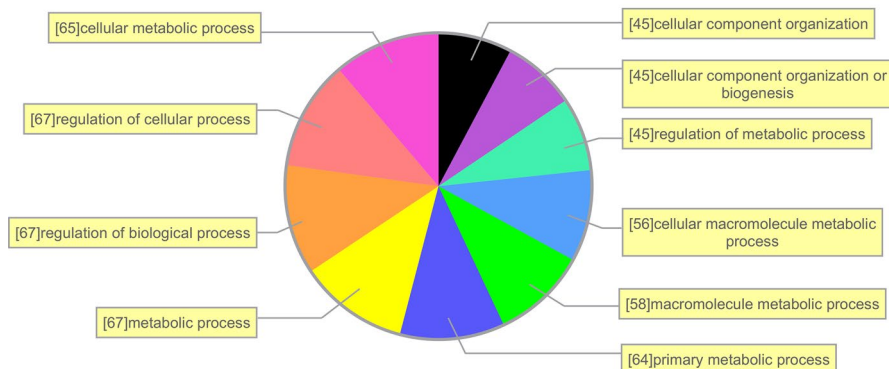


FIGURE 2 Function prediction of upregulated circRNAs in AGA (GO) enrichment analysis. Biological processes (BPs)

3 | RESULTS

3.1 | Differentially expressed circRNAs between AGA patients and healthy controls

The expression profile of circRNAs in AGA patients and that in patients in the normal control (NC) group were analyzed by fold change to determine statistical significance ($p < 0.05$). In total, 100 circRNAs were significantly upregulated, and 184 circRNAs were significantly downregulated (Figure 1A,B and Table 1). Among the 284 differentially expressed circRNAs, 213 (75%) were circular exonic RNAs, accounting for 75% (Figure 1C).

3.2 | Functions of differentially expressed circRNAs in AGA

Gene ontology and KEGG analysis were conducted after source gene analysis. GO analysis was used to explore the top 10 predictive

functions of the 284 differentially expressed circRNAs in AGA patients. GO enrichment analysis of source genes mainly includes biological processes (BPs), cellular components (CCs) and molecular functions (MFs). We identified the top 10 GO items that were significantly different between the AGA group and the NC group (Figures 2–4), with mitotic cell cycle as the top BP (Figure 2), intracellular organelle as the top CC (Figure 3), and ubiquitin-like protein ligase activity as the top MF (Figure 4). The pie chart in Figures 2–4 shows the proportion of each GO item.

3.3 | KEGG analysis indicated that the DNA replication pathway plays a key role in the pathogenesis of AGA.

Kyoto Encyclopedia of Genes and Genomes analysis allows the identification of the regulatory function of differentially expressed circRNAs by locating the pathways related to source genes. The molecular data sets for genomics, transcriptomics, protein genomics

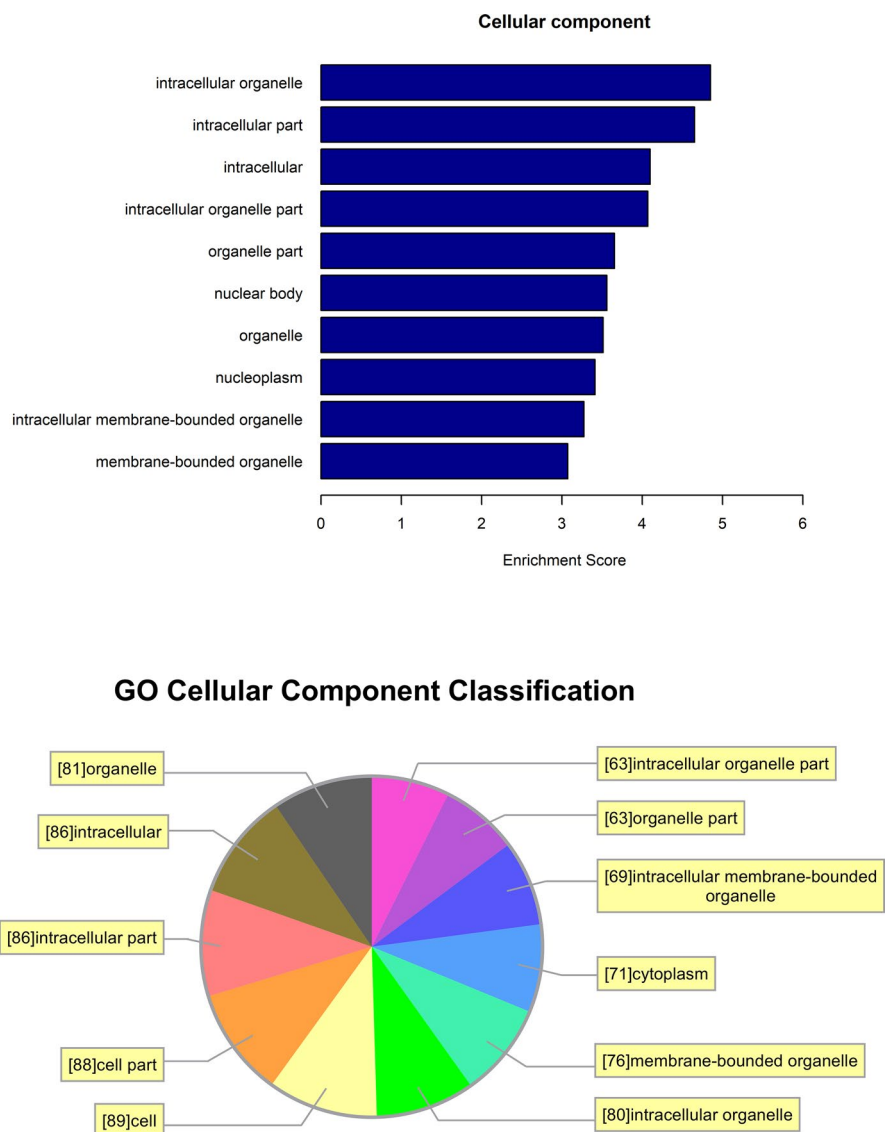


FIGURE 3 Function prediction of upregulated circRNAs in AGA (GO) enrichment analysis. Cellular components(CCs)

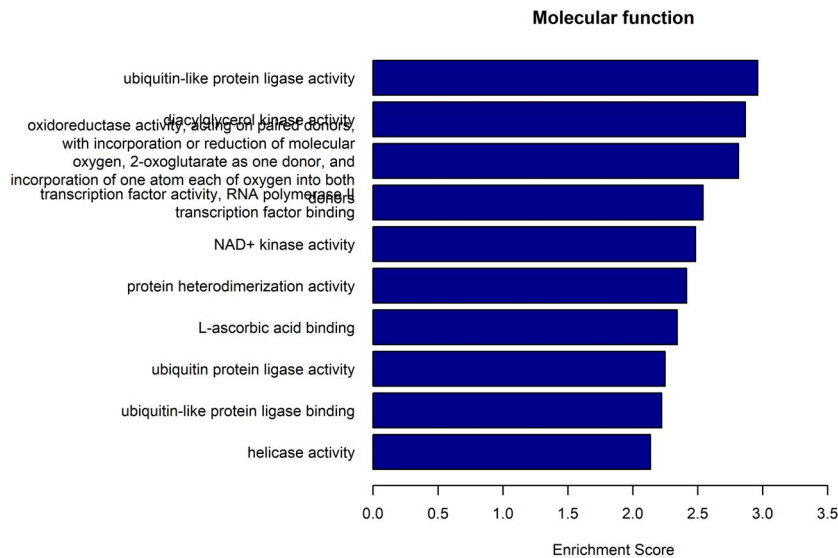
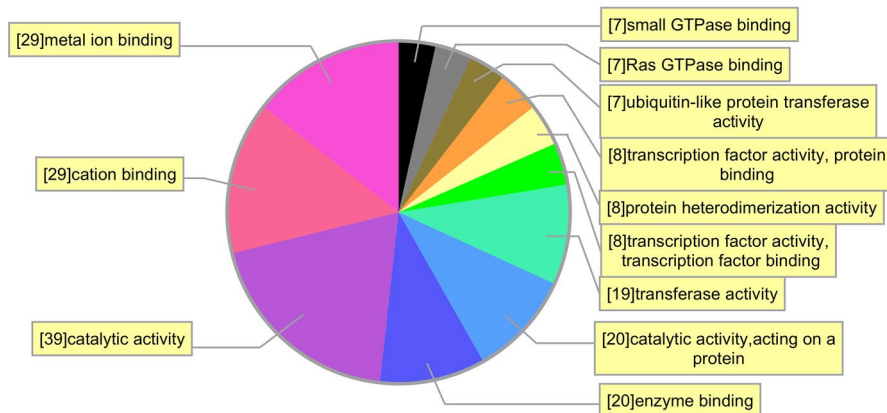


FIGURE 4 Function prediction of upregulated circRNAs in AGA (GO) enrichment analysis. Molecular functions (MFs)

GO Molecular Function Classification



and metabolomics are mapped to KEGG pathways to clarify the biological functions of molecules. In this study, function-related pathways involving 100 upregulated circRNAs in the AGA group were examined by KEGG analysis. For the AGA group, DNA replication was the most prevalent pathway enriched with differentially expressed circRNAs (Figure 5).

3.4 | Top 10 circRNAs with significantly high expression in the AGA group and control group.

We explored the interaction between differentially expressed circRNAs in the AGA group and miRNAs to evaluate the potential functions of differentially expressed circRNAs in AGA. Based on enrichment degree, TargetScan and miRanda were used to investigate the regulation of the dermal papilla cell cycle by differentially expressed circRNAs in the AGA group through miRNAs. Figure 6 provides a network diagram generated by Cytoscape software. There were many interactions between circRNAs and miRNAs, and genes related to apoptosis or alopecia (red) were closely related to differentially expressed circRNAs in the AGA group (Figure 6).

Using the hair follicles of 30 AGA patients and 30 healthy volunteers, 10 highly expressed circRNAs in the AGA group were selected, and their expression levels in large samples were verified by qRT-PCR. Among them, the difference in expression of 8 circRNAs was statistically significant ($p < 0.05$) (Figure 7), indicating that the sequencing results were reliable.

3.5 | ROC analysis showed hsa_circ_0001079 had better diagnostic value.

Receiver operating characteristic curve analysis of circRNAs with a confirmed role in AGA was carried out to evaluate the potential diagnostic value of these circRNAs. The ROC of confirmed circRNAs showed that among the 8 circRNAs, the levels of hsa_circ_0001079, hsa_circ_0002980 and hsa_circ_0005974 distinguished AGA patients from NCs. The area under the curve (AUC) was the largest for hsa_circ_0001079 (AUC 0.72, 95% CI 0.57–0.84, $p = 0.008$), followed by hsa_circ_0002980 (AUC 0.64, 95% CI 0.54–0.81, $p = 0.02$). Therefore, hsa_circ_0001079, as a biomarker for the diagnosis of AGA, might be more valuable than the other 2 circRNAs (Figure 8).

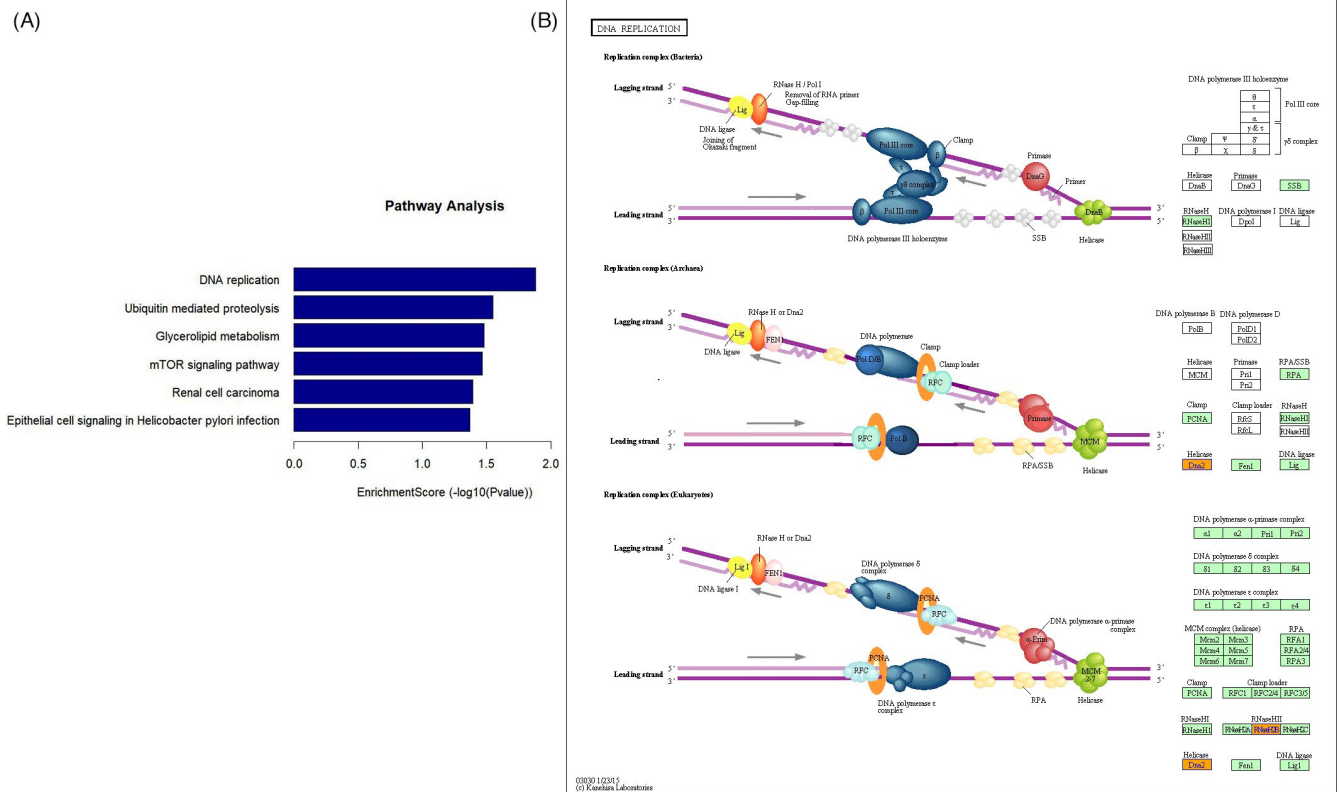
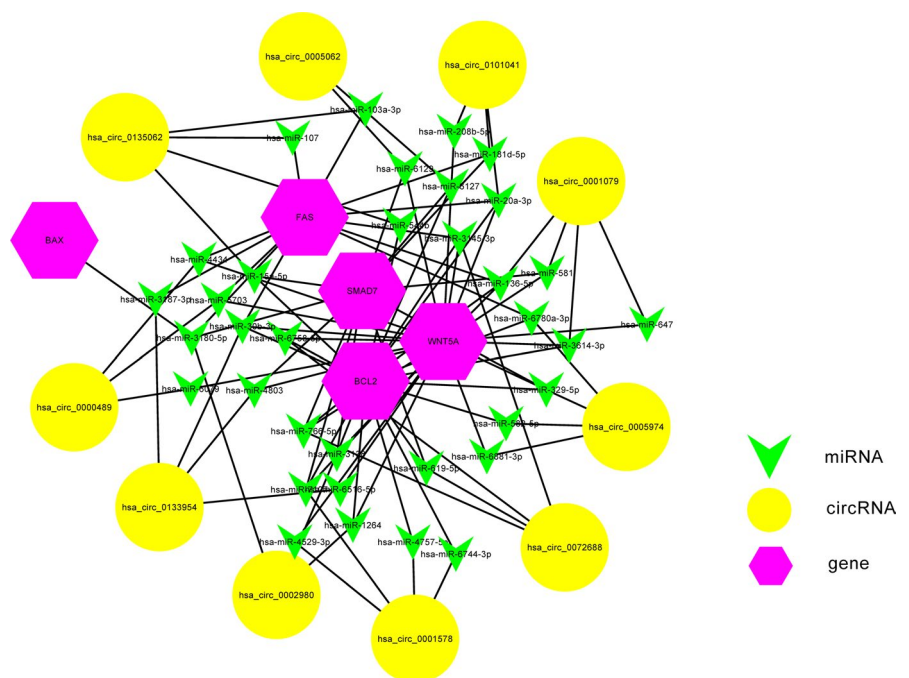


FIGURE 5 KEGG analysis indicated that the DNA replication pathway plays a key role in the pathogenesis of AGA. (A) KEGG analysis revealing the top 5 signaling pathways with upregulated circRNA enrichment, among which DNA replication was the most significant. (B) Genes and reaction elements involved in the DNA replication pathway

FIGURE 6 Top 10 circRNAs (yellow) with significantly high expression (based on high-throughput sequencing) in the AGA group and control group. These 10 circRNAs might regulate the target genes (red) through miRNAs (green arrows)



3.6 | Interaction between hsa_circ_0001079 and hsa-miR-136-5p in AGA.

The genomic expression site of hsa_circ_0001079 was verified by qRT-PCR and Sanger sequencing (Figure 9A). Based on the

sequencing results, hsa-miR-136-5p was expected to be the target of hsa_circ_0001079. Therefore, we studied the interaction between hsa_circ_0001079 and hsa-miR-136-5p. The matching binding sequence between hsa_circ_0001079 and hsa-miR-136-5p was explored by miRanda analysis (Figure 9B). The expression of

hsa-miR-136-5p in the AGA group was significantly lower than that in the NC group, and the expression of hsa-miR-136-5p was negatively correlated with that of hsa_circ_0001079 (Figure 9C).

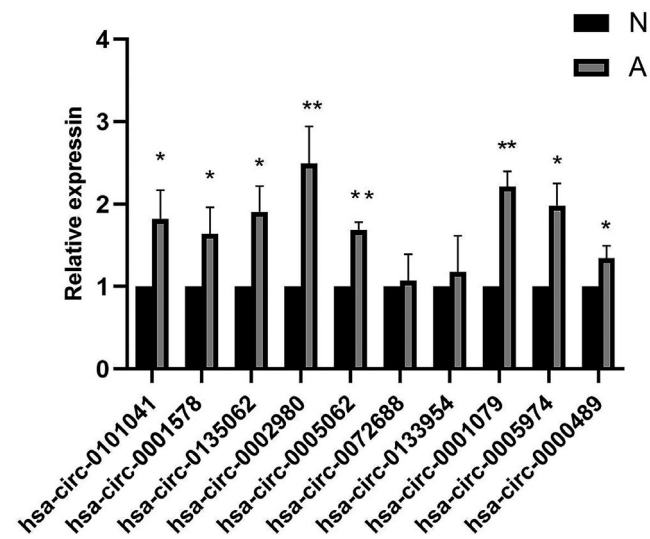
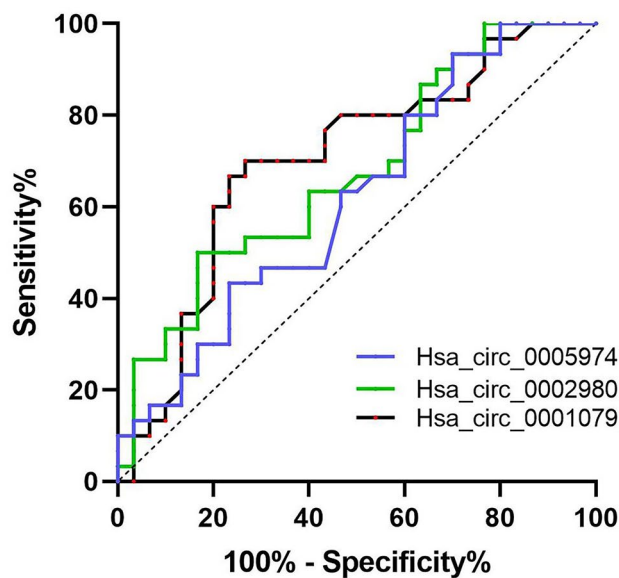


FIGURE 7 CircRNA sequencing results of samples acquired from 30 AGA patients and 30 normal volunteers were verified by qRT-PCR. In a comparison of the 2 groups, 8 circRNAs in the AGA group were significantly upregulated (* $p < 0.05$, ** $p < 0.01$)



Variables	AUC	P value	SEM	95%C.I	Sensitivity	Specificity
Has_circ_0001079	0.7211	0.0075	0.06920	0.5655- 0.8367	62.17	74.51
Has_circ_0002980	0.6427	0.0207	0.06927	0.5381- 0.8097	58.23	35.79
Has_circ_0005974	0.6178	0.1171	0.07256	0.4756- 0.7600	53.91	58.95

3.7 | The relationship between wnt5A and hsa-miR-136-5p

The matching binding sequence between Wnt5A and hsa-miR-136-5p was explored by miRanda analysis (Figure 10A). The luciferase assay showed that transfection of hsa-miR-136-5p mimics significantly reduced the relative luciferase activity of Wnt5a-WT-treated cells, but did not affect that of Wnt5a-MUT-treated cells (Figure 10B). Pearson correlation analysis showed a negative correlation between the expression level of Wnt5A and hsa-miR-136-5p in 30 AGA patients (Figure 10C).

4 | DISCUSSION

Currently, the widely recognized pathogenesis of AGA involves the specific binding of androgen and its metabolites to the androgen receptor (AR) on hair follicle cells to regulate gene transcription and protein expression in hair follicle cells, thus affecting hair growth and loss.^{1,17,18} However, the upstream regulation mechanism is still unclear. Therefore, it is necessary to determine novel biomarkers and explore their functions. In nature, hair follicles do not exist only in humans. CircRNA expression profiles have been explored in hair follicle specimens from sheep¹⁹ and rabbits.²⁰

FIGURE 8 ROC analysis showing that the expression of hsa_circ_0001079, hsa_circ_0002980 and hsa_circ_0005974 had potential significance for the diagnosis of AGA, among which hsa_circ_0001079 had better diagnostic value

(A)



(B)

2D Structure	Local AU	Position	Conservation	Predicted By
198 5' - ctgGTCATGA ^{16 15 14 13} AATTACTAA ^{7 6 5 4 3 2} GTGGAG - 3' hsa_circ_0001079 3' - aggUAGUAGUU - -UG - UU ^{7 6 5 4 3 2} UACCUCa - 5' hsa-miR-136-5p 3' pairing Seed Imperfect match	GTGGAG Imperfect			
259 5' - gaggagAACACAA - GAATGGAGt - 3' hsa_circ_0001079 3' - agguag ^{16 15 14 13} UAGUUUUGUU ^{7 6 5 4 3 2} UACCUCa - 5' hsa-miR-136-5p 3' pairing Seed 7mer-m8	AATGGAG 7mer-m8			

(C)

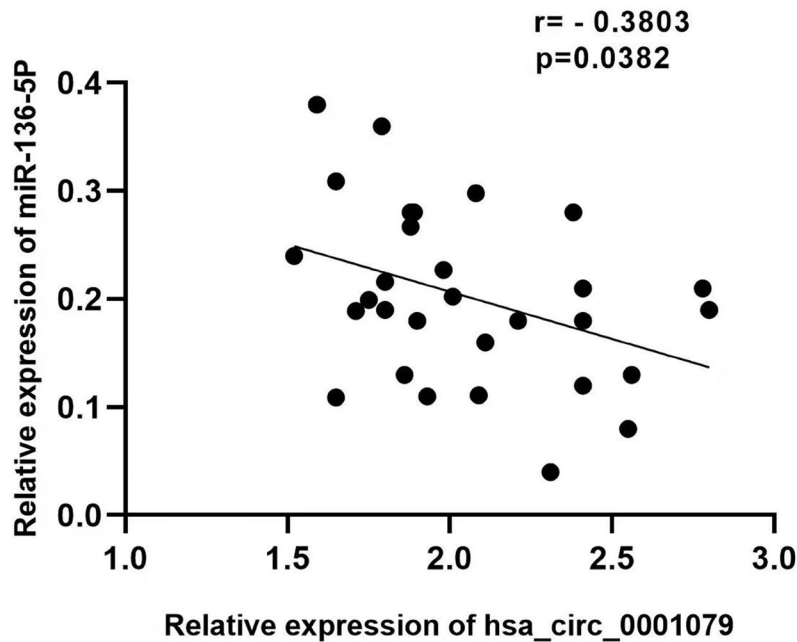


FIGURE 9 Interaction between hsa_circ_0001079 and hsa-miR-136-5p in AGA. (A) Genomic expression site and sequencing of hsa_circ_0001079. (B) Binding sequence of hsa_circ_0001079 matched with hsa-miR-136-5p (C) In the AGA group, the expression of hsa-miR-136-5p was negatively correlated with that of hsa_circ_0001079 ($p = 0.0382$)

However, it is still unclear how circRNAs play a regulatory role in human hair follicles. In the field of plastic surgery and dermatology, the growing and younger AGA population has attracted much attention. Therefore, it is of great significance to study the expression profile of AGA circRNAs and determine novel biomarkers to provide new directions and strategies for the diagnosis and treatment of AGA.

In this study, hair follicle tissue samples from AGA patients were used as the experimental group, and those from healthy adult males were used as the control group. The expression profiles of circRNAs in the experimental group were screened by whole transcriptome technology. In a comparison of the 2 groups, there were

284 circRNAs in the experimental group with fold differences >1.5 and $p < 0.05$. Among them, 100 circRNAs were upregulated, and 184 circRNAs were downregulated, most of which were exon circRNAs, with a few intron circRNAs. The findings were consistent with the reported biological characteristics of circRNAs. KEGG enrichment analysis showed that circRNAs participated in many BPs. For example, the DNA replication pathway plays a key role in the pathogenesis of AGA.

Then, we increased the number of specimens and carried out qRT-PCR verification. We selected 10 upregulated circRNAs based on their expression distribution in each specimen. The upregulated circRNAs with the most obvious differential expression ($n = 8$)

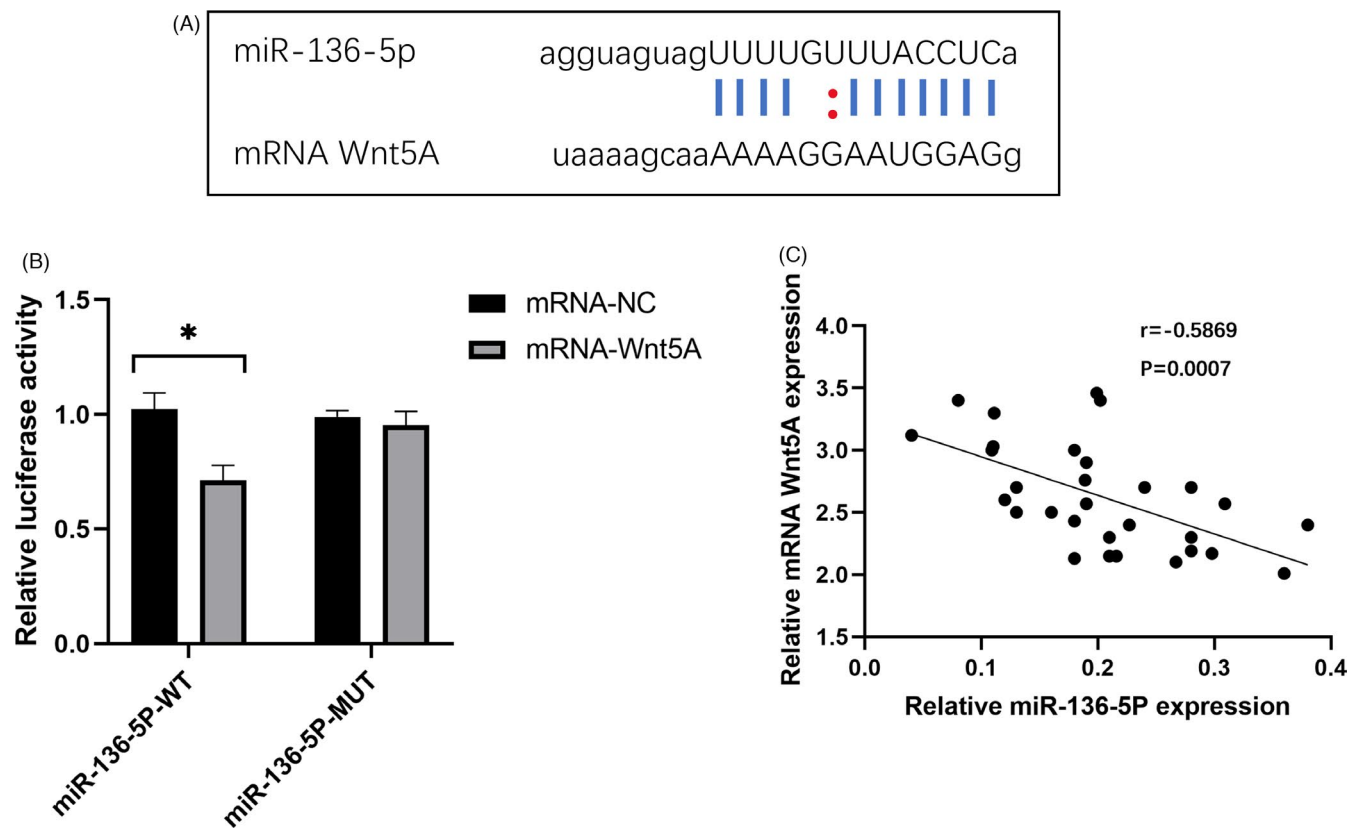


FIGURE 10 The relationship between Wnt5A and hsa-miR-136-5p. (A) The potential binding sites of Wnt5A and hsa-miR-136-5p. (B) Relative luciferase activities of wild-type (WT) and mutated (MUT) Wnt5A reporter plasmid co-transfected with hsa-miR-136-5p mimics. (C) Pearson's correlation analysis determined the relationship between Wnt5A and hsa-miR-136-5p ($p = 0.0007$)

were hsa_circ_0101041, hsa_circ_0001578, hsa_circ_0135062, hsa_circ_0002980, hsa_circ_0005062, hsa_circ_0001079, hsa_circ_0005974, and hsa_circ_0000489. ROC analysis confirmed that hsa_circ_0001079, hsa_circ_0002980 and hsa_circ_0005974 could distinguish AGA patients from NCs. Notably, hsa_circ_0001079, as a biomarker of AGA diagnosis, might have better value than the other 2 biomarkers.

The most diagnostically upregulated circRNA, hsa_circ_0001079, was studied further. Using MRE prediction software based on the TargetScan and miRanda databases, it was found that there were binding sites between hsa_circ_0001079 and hsa-miR-136-5p, and the network diagram generated by Cytoscape software showed that hsa-miR-136-5p was closely related to Wnt5A. We speculate that hsa_circ_0001079 might adsorb hsa-miR-136-5p through sponging and upregulate Wnt5A gene expression.

The hair follicle growth cycle is regulated by Wnt, Bmp, Notch and other pathways. Among them, the Wnt signaling pathway plays the most important role in regulating the hair follicle growth cycle.^{21,22} Wnt5a is a representative Wnt family protein in the non-classical Wnt pathway and plays important roles in cell proliferation, differentiation, migration and movement.²³ The non-classical Wnt5a-Cdc42 axis antagonizes classical Wnt signaling and ultimately induces a phenotype in young hair follicle stem cells similar to premature aging.^{24,25} To understand the role of the Wnt signaling pathway in hair follicle growth,

when locating Wnt marker proteins, it was found that Wnt10b and TCF3 were highly expressed in dermal papilla cells during the growth period, while Wnt5a and Wnt10a were weakly expressed.²⁶ In addition, the overexpression of Wnt5a can promote the degradation of β -catenin, inhibit the activation of the classical Wnt/ β -catenin pathway, delay hair follicle growth from the static phase to growth phase, and inhibit hair follicle growth.^{27,28} All these findings indicate that Wnt5a is an important gene for inhibiting hair follicle growth. This fit well with our research hypothesis, that is, in AGA, hsa_circ_0001079 overexpression upregulates Wnt5A expression and inhibits hair growth by adsorbing hsa-miR-136-5p.

In previous studies, when we identified the regulatory function of differentially expressed circRNAs by locating the pathways related to the source genes via KEGG analysis, we found that DNA replication was the most obvious pathway for enriching differentially expressed circRNAs in AGA. Related studies have shown that with the increase in Wnt5A expression, the expression of cyclin D1 and the replication of DNA increase in the cell cycle of mesenchymal stem cells under mechanical strain and in the natural growth of mouse mandibular condyle.²⁹ Self-renewing adipose-derived mesenchymal stem cells continuously mediate DNA replication, chromatin packaging, cell structure expansion and mitosis, regulate Wnt signal components, and upregulate Wnt5A-related genes such as WISP2, SFRP2, and SFRP4.³⁰ In the progression of prostate cancer,

Wnt5A and DNA replication have the same expression trends.³¹ These studies have revealed that the DNA replication pathway, as determined by KEGG analysis, is closely related to Wnt5A. Combined with the hypothesis that hsa_circ_0001079 targets Wnt5A by adsorbing hsa-miR-136-5p, we further speculated that hsa_circ_0001079 mediated hair loss by regulating Wnt5A.

In future, more functions of differentially expressed circRNAs will be explored in large-sample data. The relationship between hsa_circ_0001079 and AGA in this study suggests that hsa_circ_0001079 plays a key role in the occurrence and development of AGA. The reverse correlation and perfect binding sequence between hsa_circ_0001079 and miR-136-5p suggests that hsa_circ_0001079 might regulate Wnt5A mRNA to inhibit normal hair follicle growth through sponging adsorption of miR-136-5p and that Wnt5A also participates in multiple cellular DNA replication pathways. Next, we need to carry out further cell and animal model experiments to deepen our understanding of the specific mechanism and function of circRNAs in AGA.

CONFLICT OF INTEREST

The authors declared no potential conflicts of interest with respect to the research, authorship, or publication of this article.

AUTHOR CONTRIBUTIONS

All authors participated in the design, interpretation of the studies and analysis of the data and review of the manuscript.

DATA AVAILABILITY STATEMENT

The data that support the findings of this study are available from the corresponding author upon reasonable request.

ORCID

Xiaoyu Xu  <https://orcid.org/0000-0002-2377-5330>

REFERENCES

- Kozicka K, Łukasik A, Jaworek A, et al. The level of stress and the assessment of selected clinical parameters in patients with androgenetic alopecia. *Pol Merkuri Lekarski*. 2020;48(288):427-430.
- Wang ZD, Feng Y, Sun L, et al. Anti-androgenetic alopecia effect of policosanol from Chinese wax by regulating abnormal hormone levels to suppress premature hair follicle entry into the regression phase. *Biomed Pharmacother*. 2021;136:111241.
- Vasudevan B, Neema S, Ghosh K, Singh S, Khera A. Hair transplantation by follicular unit extraction for male androgenetic alopecia: a retrospective observational study from two centers. *Med J Armed Forces India*. 2020;76(4):430-437.
- Hooper D. Platelet-rich plasma has a place in the treatment of androgenetic alopecia. *J Am Acad Dermatol*. 2021;84(4):1186-1187.
- Steward EN, Patel H, Pandya H, et al. Efficacy of platelet-rich plasma and concentrated growth factor in treating androgenetic alopecia - A retrospective study. *Ann Maxillofac Surg*. 2020;10(2):409-416.
- Gentile P. Autologous cellular method using micrografts of human adipose tissue derived follicle stem cells in androgenetic alopecia. *Int J Mol Sci*. 2019;20(14):3446.
- Irfan MM, Shah SU, Khan IU, et al. Physicochemical characterization of finasteride nanosystem for enhanced topical delivery. *Int J Nanomed*. 2021;16:1207-1220.
- Khera M, Than JK, Anaissie J, et al. Penile vascular abnormalities in young men with persistent side effects after finasteride use for the treatment of androgenic alopecia. *Transl Androl Urol*. 2020;9(3):1201-1209.
- Li Z, Ruan Y, Zhang H, Shen Y, Li T, Xiao B. Tumor-suppressive circular RNAs: Mechanisms underlying their suppression of tumor occurrence and use as therapeutic targets. *Cancer Sci*. 2019;110(12):3630-3638.
- Lu Y, Li Z, Lin C, Zhang J, Shen Z. Translation role of circRNAs in cancers. *J Clin Lab Anal*. 2021;35(7):e23866.
- Robic A, Kuhn C. Beyond Back Splicing, a Still Poorly Explored World: Non-Canonical Circular RNAs. *Genes (Basel)*. 2020;11(9):1111.
- Panda AC. Circular RNAs act as miRNA sponges. *Adv Exp Med Biol*. 2018;1087:67-79.
- Zhou C, Liu HS, Wang FW, et al. CircCAMSAP1 promotes tumor growth in colorectal cancer via the miR-328-5p/E2F1 axis. *Mol Ther*. 2020;28(3):914-928.
- Wen Y, Chun Y, Lian ZQ, et al. circRNA-0006896-miR1264-DNMT1 axis plays an important role in carotid plaque destabilization by regulating the behavior of endothelial cells in atherosclerosis. *Mol Med Rep*. 2021;23:5.
- Xi P, Zhang CL, Wu SY, Liu L, Li WJ, Li YM. CircRNA circ-IQGAP1 knockdown alleviates interleukin-1 β -induced osteoarthritis progression via targeting miR-671-5p/TCF4. *Orthop Surg*. 2021;13(3):1036-1046.
- Zhang W, Zhang C, Hu C, Luo C, Zhong B, Yu X. Circular RNA-CDR1as acts as the sponge of microRNA-641 to promote osteoarthritis progression. *J Inflamm (Lond)*. 2020;17:8.
- Motofei IG, Rowland DL, Tampa M, et al. Finasteride and androgenic alopecia; from therapeutic options to medical implications. *J Dermatolog Treat*. 2020;31(4):415-421.
- Martinez-Lopez A, Montero-Vilchez T, Sierra-Sanchez A, Molina-Leyva A, Arias-Santiago S. Advanced medical therapies in the management of non-scarring alopecia: areata and androgenic alopecia. *Int J Mol Sci*. 2020;21(21):8390.
- Yin RH, Zhao SJ, Jiao Q, et al. CircRNA-1926 promotes the differentiation of goat SHF stem cells into hair follicle lineage by miR-148a/b-3p/CDK19 axis. *Animals (Basel)*. 2020;10(9):1552.
- Zhao B, Chen Y, Hu S, et al. Systematic analysis of non-coding RNAs involved in the Angora Rabbit (*Oryctolagus cuniculus*) hair follicle cycle by RNA sequencing. *Front Genet*. 2019;10:407.
- Choi BY. Targeting Wnt/ β -Catenin pathway for developing therapies for hair loss. *Int J Mol Sci*. 2020;21(14):4915.
- Hawkshaw NJ, Hardman JA, Alam M, Jimenez F, Paus R. Deciphering the molecular morphology of the human hair cycle: Wnt signaling during the telogen-anagen transformation. *Br J Dermatol*. 2020;182(5):1184-1193.
- Su Y, Wen J, Zhu J, et al. Pre-aggregation of scalp progenitor dermal and epidermal stem cells activates the WNT pathway and promotes hair follicle formation in in vitro and in vivo systems. *Stem Cell Res Ther*. 2019;10(1):403.
- Tiwari RL, Mishra P, Martin N, et al. A Wnt5a-Cdc42 axis controls aging and rejuvenation of hair-follicle stem cells. *Aging (Albany NY)*. 2021;13(4):4778-4793.
- Avigad Laron E, Aamar E, Enshell-Seijffers D. The mesenchymal niche of the hair follicle induces regeneration by releasing primed progenitors from inhibitory effects of quiescent stem cells. *Cell Rep*. 2018;24(4):909-921.e903.
- Lin CM, Yuan YP, Chen XC, et al. Expression of Wnt/ β -catenin signaling, stem-cell markers and proliferating cell markers in rat whisker hair follicles. *J Mol Histol*. 2015;46(3):233-240.
- Xing Y, Ma X, Guo H, Deng F, Yang J, Li Y. Wnt5a suppresses β -catenin signaling during hair follicle regeneration. *Int J Med Sci*. 2016;13(8):603-610.
- Chen X, Liu B, Li Y, et al. Dihydrotestosterone regulates hair growth through the Wnt/ β -Catenin pathway in C57BL/6 mice and in vitro organ culture. *Front Pharmacol*. 2019;10:1528.

29. Al-kalaly A, Wu C, Wong R, Rabie AB. The assessment of cell cycle genes in the rat mandibular condyle. *Arch Oral Biol*. 2009;54(5):470-478.
30. Dudakovic A, Camilleri E, Riester SM, et al. High-resolution molecular validation of self-renewal and spontaneous differentiation in clinical-grade adipose-tissue derived human mesenchymal stem cells. *J Cell Biochem*. 2014;115(10):1816-1828.
31. Hruby E, Vondracek J, Libalova H, et al. Gene expression changes in human prostate carcinoma cells exposed to genotoxic and nongenotoxic aryl hydrocarbon receptor ligands. *Toxicol Lett*. 2011;206(2):178-188.

How to cite this article: Wei H, Xu X, Yang S, Liu C, Li Q, Jin P. The potential role of hsa_circ_0001079 in androgenetic alopecia via sponging hsa-miR-136-5p. *J Clin Lab Anal*. 2022;36:e24021. doi:[10.1002/jcla.24021](https://doi.org/10.1002/jcla.24021)